

Overview of OpenMX:

Implementation and practical aspects

1. Introduction

2. Implementation

Total energy, forces, numerical integrations,
basis functions, getting SCF, geometry optimization,
parallelization, codes.

3. Ongoing and planned works

4. Summary

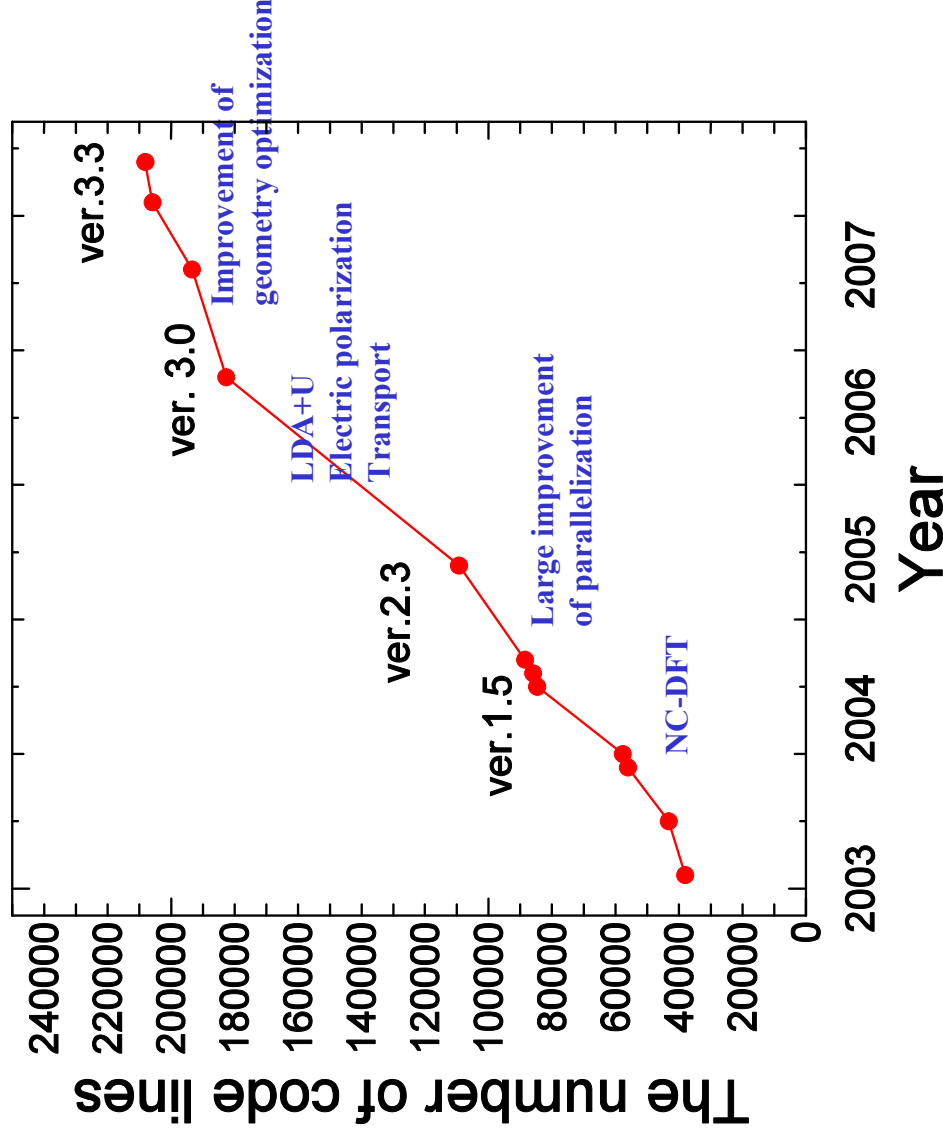
Short history of OpenMX

The development of the code has been **started** from the middle of **2000**.

The first public release was done at 2003 January, and **thirteen releases** were made **until now**.

The code has been steadily developed as shown the figure, and the community itself has been also growing.

The number of lines of the code



Contributors

- T. Ozaki (JAIST)
- H. Kino (NIMS)
- J. Yu (SNU)
- M. J. Han(UC,Davis)
- N. Kobayashi (Tsukuba Univ.)
- M. Ohfuti (Fujitsu)
- F. Ishii (Kanazawa Univ.)
- T. Ohwaki (Nissan)
- H. Weng (JAIST)
- K. Terakura (JAIST)

OpenMX Open source package for Material eXplorer

OpenMX is based on LDA, GGA, LDA+U, local pseudo-atomic basis functions, and norm-conserving pseudopotentials. The memory requirement scales as $O(N)$, and the computational cost is proportional to the third power of number of atoms or linearly.

Hamiltonian matrix

$O(N)$ operations

LDA or GGA

Separable pseudo potentials

Numerical atomic basis

Real space grids integration

Database of basis and pseudo potentials

Poisson's equation Eigenvalue problem

$O(N \log(N))$ operations

Fast Fourier transform

$O(N^3)$ operations

Conventional diagonalization

$O(N)$ operations

Krylov subspace

Divide-Conquer

Features of Ver. 3.3

Magnetism

collinear, non-collinear DFT
spin-orbit coupling
orbital magnetic moment
LDA+U
exchange coupling J
constraint DFT with SNU

Electric polarization

polarization by Berry phase
Born effective charge

with Dr. Ishii

Eigenvalue problem

O(N)
Band
Cluster
NEGF

MD or Geo. opt.

NEV
NTV
Steepest decent
EF, RF, BFGS, DIIS

Electric transport

NEGF calc. with a finite bias
transmission
I-V curve

with NIMS and Prof. Kobayashi

Optical properties

optical conductivity

with NIMS

Implementation of OpenMX

- **Total energy**
- **Numerical integration**
- **Forces**
- **Basis functions**
- **Getting SCF**
- **Geometry optimization**
- **Parallelization**
- **Handling of the code**

Total energy No.1

The total energy is given by that of the conventional DFT. The reorganization of the Coulomb energies is a key for the accurate implementation

$$E_{\text{tot}} = E_{\text{kin}} + E_{\text{ec}} + E_{\text{ee}} + E_{\text{xc}} + E_{\text{cc}}.$$

$$E_{\text{kin}} = \sum_{\sigma} \sum_{i\alpha, j\beta}^N \rho_{\sigma, i\alpha j\beta}^{(\mathbf{R}_n)} h_{i\alpha j\beta, \text{kin}}^{(\mathbf{R}_n)}.$$

$$E_{\text{ec}} = E_{\text{ec}}^{(\text{L})} + E_{\text{ec}}^{(\text{NL})},$$

$$= \sum_{\sigma} \sum_{i\alpha, j\beta}^N \rho_{\sigma, i\alpha j\beta}^{(\mathbf{R}_n)} \langle \phi_{i\alpha}(\mathbf{r} - \tau_i) | \sum_I V_{\text{core}, I}(\mathbf{r} - \tau_I) | \phi_{j\beta}(\mathbf{r} - \tau_j - \mathbf{R}_n) \rangle$$

$$+ \sum_{\sigma} \sum_{i\alpha, j\beta}^N \rho_{\sigma, i\alpha j\beta}^{(\mathbf{R}_n)} \langle \phi_{i\alpha}(\mathbf{r} - \tau_i) | \sum_I V_{\text{NL}, I}(\mathbf{r} - \tau_I) | \phi_{j\beta}(\mathbf{r} - \tau_j - \mathbf{R}_n) \rangle,$$

$$E_{\text{ee}} = \frac{1}{2} \int d\mathbf{r}^3 n(\mathbf{r}) V_{\text{H}}(\mathbf{r}),$$

$$= \frac{1}{2} \int d\mathbf{r}^3 n(\mathbf{r}) \{ V_{\text{H}}^{(\text{a})}(\mathbf{r}) + \delta V_{\text{H}}(\mathbf{r}) \},$$

$$E_{\text{xc}} = \int d\mathbf{r}^3 \{ n_{\uparrow}(\mathbf{r}) + n_{\downarrow}(\mathbf{r}) + n_{\text{pcc}}(\mathbf{r}) \} \epsilon_{\text{xc}}(n_{\uparrow} + \frac{1}{2}n_{\text{pcc}}, n_{\downarrow} + \frac{1}{2}n_{\text{pcc}}),$$

$$E_{\text{cc}} = \frac{1}{2} \sum_{I, J} \frac{Z_I Z_J}{|\tau_I - \tau_J|}.$$

Total energy No.2

The reorganization of Coulomb energies gives **three new energy terms**.

$$E_{\text{ec}}^{(L)} + E_{\text{ee}} + E_{\text{cc}} = E_{\text{na}} + E_{\delta\text{ee}} + E_{\text{ecc}},$$

The neutral atom energy

$$\begin{aligned} E_{\text{na}} &= \int dr^3 n(\mathbf{r}) \sum_I V_{\text{na},I}(\mathbf{r} - \tau_I), \\ &= \sum_{\sigma} \sum_{\mathbf{n}} \sum_{i\alpha,j\beta} \rho_{\sigma,i\alpha,j\beta}^{(\mathbf{R}_n)} \sum_I \langle \phi_{i\alpha}(\mathbf{r} - \tau_i) | V_{\text{na},I}(\mathbf{r} - \tau_I) | \phi_{j\beta}(\mathbf{r} - \tau_j - \mathbf{R}_n) \rangle, \end{aligned}$$

Difference charge Hartree energy

$$E_{\delta\text{ee}} = \frac{1}{2} \int dr^3 \delta n(\mathbf{r}) \delta V_{\text{H}}(\mathbf{r}),$$

Screened core-core repulsion energy

$$E_{\text{scc}} = \frac{1}{2} \sum_{I,J} \left[\frac{Z_I Z_J}{|\tau_I - \tau_J|} - \int dr^3 n_I^{(a)}(\mathbf{r}) V_{\text{H},J}^{(a)}(\mathbf{r}) \right].$$

Difference charge

$$\begin{aligned} \delta n(\mathbf{r}) &= n(\mathbf{r}) - n^{(a)}(\mathbf{r}), \\ &= n(\mathbf{r}) - \sum_i n_i^{(a)}(\mathbf{r}), \end{aligned}$$

Neutral atom potential

$$V_{\text{na},I}(\mathbf{r} - \tau_I) = V_{\text{core},I}(\mathbf{r} - \tau_I) + V_{\text{H},I}^{(a)}(\mathbf{r} - \tau_I).$$

Total energy No.3

So, the total energy is given by

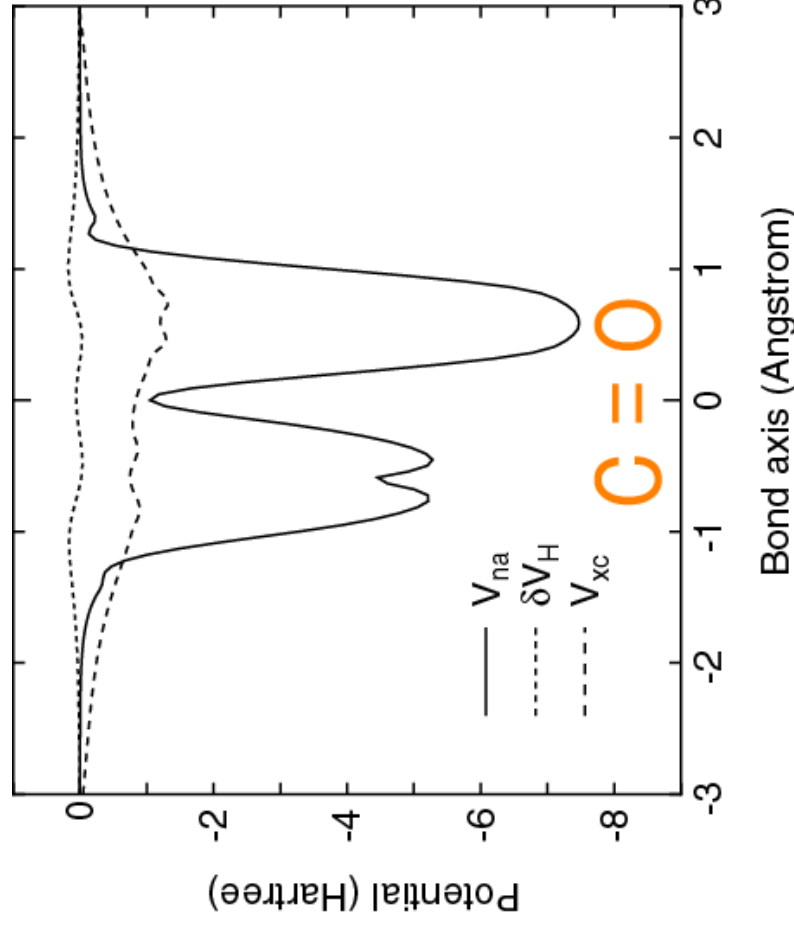
$$E_{\text{tot}} = E_{\text{kin}} + E_{\text{na}} + E_{\text{ec}}^{(\text{NL})} + E_{\delta\text{ee}} + E_{\text{xc}} + E_{\text{scc}}.$$

Each term is evaluated by using a different numerical grid.

E_{kin}	}	Spherical coordinate in momentum space
E_{na}		
$E_{\text{ec}}^{(\text{NL})}$		
$E_{\delta\text{ee}}$	}	Real space regular mesh
E_{xc}		
E_{scc}		Real space fine mesh

Projector expansion of V_{na} No.1

V_{na} tends to be very **deep**, leading to a serious numerical problem.



$$V_{\text{eff}} = \sum_k V_{\text{NL},k} + \sum_k V_{\text{na},k} + \delta V_{\text{H}} + V_{\text{xc}},$$

V_{na} can be expanded by projectors:

$$\hat{V}_{\text{na},k} = \sum_{lm}^{L_{\text{max}}} \sum_{\zeta}^{N_{\text{rad}}} |V_{\text{na},k} \bar{R}_{l\zeta} Y_{lm}\rangle \frac{1}{c_{l\zeta}} \langle Y_{lm} \bar{R}_{l\zeta} V_{\text{na},k} |,$$

where a set of radial functions $\{R_{l\zeta}\}$ is an orthonormal set defined by a norm $\int r^2 dr R_{l\zeta} V_{\text{na},k} R_{l\zeta}'$ for radial functions R and R' , and is calculated by the following Gram-Schmidt orthogonalization:

$$\bar{R}_{l\zeta} = R_{l\zeta} - \sum_{\eta}^{\zeta-1} \bar{R}_{l\eta} \frac{1}{c_{l\eta}} \int r^2 dr \bar{R}_{l\eta} V_{\text{na},k} R_{l\zeta},$$

$$c_{l\zeta} = \int r^2 dr \bar{R}_{l\zeta} V_{\text{na},k} \bar{R}_{l\zeta}.$$

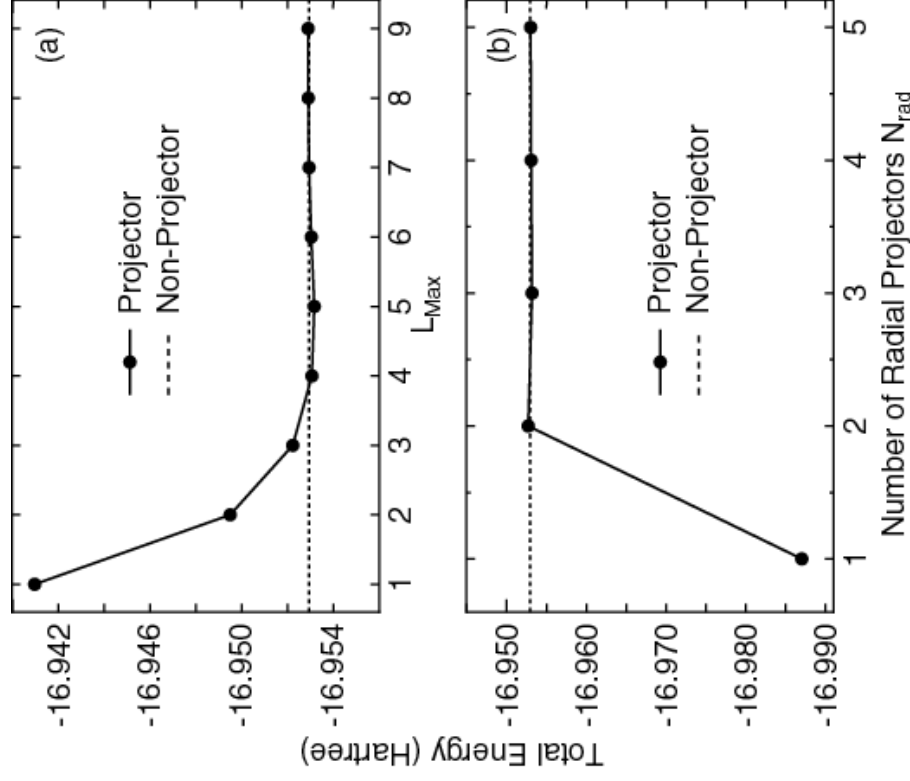
TO and H.Kino, PRB 72, 045121 (2005)

Three center integrals with V_{na} can be transformed to products of two center integrals by the projector expansion method.

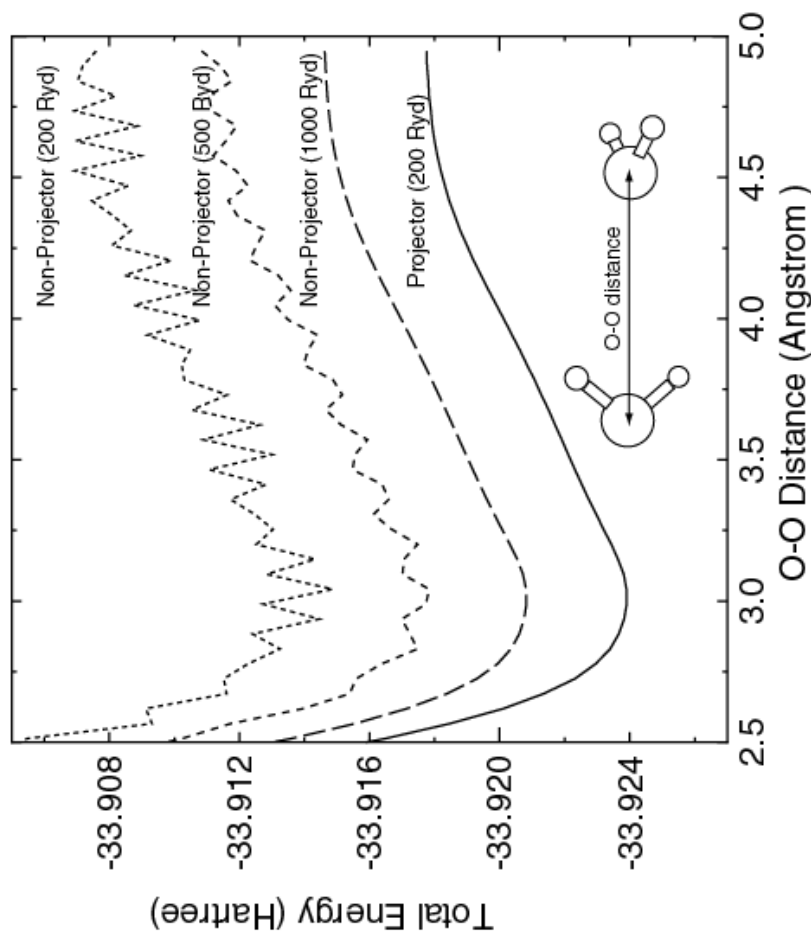
Projector expansion of V_{na} No.2

Convergence properties

$$\hat{V}_{na,k} = \sum_{\zeta}^{L_{\max}, N_{\text{rad}}} \sum_{lm} |V_{na,k} \bar{R}_{l\zeta} Y_{lm}\rangle \frac{1}{c_{l\zeta}} \langle Y_{lm} \bar{R}_{l\zeta} V_{na,k} |,$$



Comparison between non-projector and projector methods



Two center integrals

Fourier-transformation of basis functions

$$\begin{aligned}
 \tilde{\phi}_{i\alpha}(\mathbf{k}) &= \left(\frac{1}{\sqrt{2\pi}}\right)^3 \int d\mathbf{r}^3 \phi_{i\alpha}(\mathbf{r}) e^{-i\mathbf{k}\cdot\mathbf{r}} \\
 &= \left(\frac{1}{\sqrt{2\pi}}\right)^3 \int d\mathbf{r}^3 Y_{lm}(\hat{\mathbf{r}}) R_{pl}(\mathbf{r}) \left\{ 4\pi \sum_{L=0}^{\infty} \sum_{M=-L}^L (-i)^L j_L(kr) Y_{LM}(\hat{\mathbf{k}}) Y_{LM}^*(\hat{\mathbf{r}}) \right\}, \\
 &= \left(\frac{1}{\sqrt{2\pi}}\right)^3 4\pi \sum_{L=0}^{\infty} \sum_{M=-L}^L (-i)^L Y_{LM}(\hat{\mathbf{k}}) \int d\mathbf{r} r^2 R_{pl}(\mathbf{r}) j_L(kr) \int d\theta d\phi \sin(\theta) Y_{lm}(\hat{\mathbf{r}}) Y_{LM}^*(\hat{\mathbf{r}}), \\
 &= \left[\left(\frac{1}{\sqrt{2\pi}}\right)^3 4\pi (-i)^l \int d\mathbf{r} r^2 R_{pl}(\mathbf{r}) j_L(kr)\right] Y_{lm}(\hat{\mathbf{k}}), \\
 &= \tilde{R}_{pl}(k) Y_{lm}(\hat{\mathbf{k}}),
 \end{aligned}$$

e.g., overlap integral

$$\begin{aligned}
 \langle \phi_{i\alpha}(\mathbf{r}) | \phi_{j\beta}(\mathbf{r} - \boldsymbol{\tau}) \rangle &= \int d\mathbf{r}^3 \phi_{i\alpha}^*(\mathbf{r}) \phi_{j\beta}(\mathbf{r} - \boldsymbol{\tau}), \\
 &= \int d\mathbf{r}^3 \left(\frac{1}{\sqrt{2\pi}}\right)^3 \int dk^3 \tilde{R}_{pl}^*(k) Y_{lm}^*(\hat{\mathbf{k}}) e^{-i\mathbf{k}\cdot\mathbf{r}} \left(\frac{1}{\sqrt{2\pi}}\right)^3 \int dk'^3 \tilde{R}_{p'l'}(k') Y_{l'm'}(\hat{\mathbf{k}}') e^{i\mathbf{k}'\cdot(\mathbf{r}-\boldsymbol{\tau})}, \\
 &= \left(\frac{1}{2\pi}\right)^3 \int dk^3 \int dk'^3 e^{-i\mathbf{k}'\cdot\boldsymbol{\tau}} \tilde{R}_{pl}^*(k) Y_{lm}^*(\hat{\mathbf{k}}) \tilde{R}_{p'l'}(k') Y_{l'm'}(\hat{\mathbf{k}}') \int d\mathbf{r}^3 e^{i(\mathbf{k}'-\mathbf{k})\cdot\mathbf{r}}, \\
 &= \int dk^3 e^{-i\mathbf{k}\cdot\boldsymbol{\tau}} \tilde{R}_{pl}^*(k) Y_{lm}^*(\hat{\mathbf{k}}) \tilde{R}_{p'l'}(k) Y_{l'm'}(\hat{\mathbf{k}}), \\
 &= \int dk^3 \left[4\pi \sum_{L=0}^{\infty} \sum_{M=-L}^L (-i)^L j_L(kr) Y_{LM}(\hat{\mathbf{k}}) Y_{LM}^*(\hat{\mathbf{r}}) \right] \tilde{R}_{pl}^*(k) Y_{lm}^*(\hat{\mathbf{k}}) \tilde{R}_{p'l'}(k) Y_{l'm'}(\hat{\mathbf{k}}), \\
 &= 4\pi \sum_{L=0}^{\infty} \sum_{M=-L}^L (-i)^L Y_{LM}^*(\hat{\boldsymbol{\tau}}) C_{l(-m),l'm',LM} \int dk k^2 j_L(k|\boldsymbol{\tau}|) \tilde{R}_{pl}^*(k) \tilde{R}_{p'l'}(k),
 \end{aligned}$$

Forces

$$\begin{aligned} \mathbf{F}_i &= -\frac{\partial E_{\text{tot}}}{\partial \mathbf{R}_i} \\ &= -\frac{\partial E_{\text{kin}}}{\partial \mathbf{R}_i} - \frac{\partial E_{\text{na}}}{\partial \mathbf{R}_i} - \frac{\partial E_{\text{scc}}}{\partial \mathbf{R}_i} - \frac{\partial E_{\delta\text{ee}}}{\partial \mathbf{R}_i} - \frac{\partial E_{\text{xc}}}{\partial \mathbf{R}_i} - \frac{\partial E_{\text{cc}}}{\partial \mathbf{R}_i} \end{aligned}$$

$$\frac{\partial E_{\delta\text{ee}}}{\partial \mathbf{R}_k} = \sum_{\mathbf{p}} \frac{\partial n(\mathbf{r}_{\mathbf{p}})}{\partial \mathbf{R}_k} \frac{\partial E_{\delta\text{ee}}}{\partial n(\mathbf{r}_{\mathbf{p}})} + \sum_{\mathbf{p}} \frac{\partial n^s(\mathbf{r}_{\mathbf{p}})}{\partial \mathbf{R}_k} \frac{\partial E_{\delta\text{ee}}}{\partial n^s(\mathbf{r}_{\mathbf{p}})}$$

$$\frac{\partial E_{\delta\text{ee}}}{\partial n(\mathbf{r}_{\mathbf{p}})} = \frac{1}{2} \Delta V \{ \delta V_{\text{H}}(\mathbf{r}_{\mathbf{p}}) + \sum_{\mathbf{q}} \delta n(\mathbf{r}_{\mathbf{q}}) \frac{\partial \delta V_{\text{H}}(\mathbf{r}_{\mathbf{q}})}{\partial n(\mathbf{r}_{\mathbf{p}})} \},$$

$$= \frac{1}{2} \Delta V \{ \delta V_{\text{H}}(\mathbf{r}_{\mathbf{p}}) + \frac{4\pi}{N_{\text{rsg}}} \sum_{\mathbf{q}} \frac{1}{|\mathbf{G}|^2} \sum_{\mathbf{q}} \delta n(\mathbf{r}_{\mathbf{q}}) e^{i\mathbf{G} \cdot (\mathbf{r}_{\mathbf{q}} - \mathbf{r}_{\mathbf{p}})} \},$$

$$= \Delta V \delta V_{\text{H}}(\mathbf{r}_{\mathbf{n}}).$$

$$\frac{\partial E_{\delta\text{ee}}}{\partial n^s(\mathbf{r}_{\mathbf{p}})} = -\frac{1}{2} \Delta V \{ \delta V_{\text{H}}(\mathbf{r}_{\mathbf{p}}) - \sum_{\mathbf{q}} \delta n(\mathbf{r}_{\mathbf{q}}) \frac{\partial \delta V_{\text{H}}(\mathbf{r}_{\mathbf{q}})}{\partial n^s(\mathbf{r}_{\mathbf{p}})} \},$$

$$= -\frac{1}{2} \Delta V \{ \delta V_{\text{H}}(\mathbf{r}_{\mathbf{p}}) + \frac{4\pi}{N_{\text{rsg}}} \sum_{\mathbf{q}} \frac{1}{|\mathbf{G}|^2} \sum_{\mathbf{q}} \delta n(\mathbf{r}_{\mathbf{q}}) e^{i\mathbf{G} \cdot (\mathbf{r}_{\mathbf{q}} - \mathbf{r}_{\mathbf{p}})} \},$$

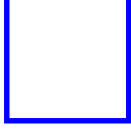
$$= -\Delta V \delta V_{\text{H}}(\mathbf{r}_{\mathbf{p}}).$$

$$\frac{\partial n(\mathbf{r}_{\mathbf{p}})}{\partial \mathbf{R}_k} = \sum_{i\alpha, j\beta} \frac{\partial c_{i\alpha, \nu}^*}{\nu} c_{j\beta, \nu} \chi_{i\alpha}(\mathbf{r}) \chi_{j\beta}(\mathbf{r}) + c_{i\alpha, \nu}^* \frac{\partial c_{j\beta, \nu}}{\partial \mathbf{R}_k} \chi_{i\alpha}(\mathbf{r}_{\mathbf{p}}) \chi_{j\beta}(\mathbf{r}_{\mathbf{p}}) \}$$

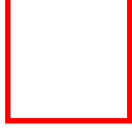
$$+ 2 \sum_{\alpha, j\beta} \rho_{k\alpha, j\beta} \frac{\partial \chi_{k\alpha}(\mathbf{r}_{\mathbf{p}})}{\partial \mathbf{R}_k} \chi_{j\beta}(\mathbf{r}_{\mathbf{p}}).$$

$$\frac{\partial E_{\text{xc}}}{\partial \mathbf{R}_k} = \sum_{\mathbf{p}} \frac{\partial n(\mathbf{r}_{\mathbf{p}})}{\partial \mathbf{R}_k} \frac{\partial E_{\text{xc}}}{\partial n(\mathbf{r}_{\mathbf{p}})},$$

$$= \Delta V \sum_{\mathbf{p}} \frac{\partial n(\mathbf{r}_{\mathbf{p}})}{\partial \mathbf{R}_k} v_{\text{xc}}(n(\mathbf{r}_{\mathbf{p}})).$$



Easy calc.



See the left

Forces are always analytic at any grid fineness and at zero temperature, even if numerical basis functions and numerical grids.

Basis functions in OpenMX

1) Primitive functions

generated by a confinement scheme

2) Optimized functions

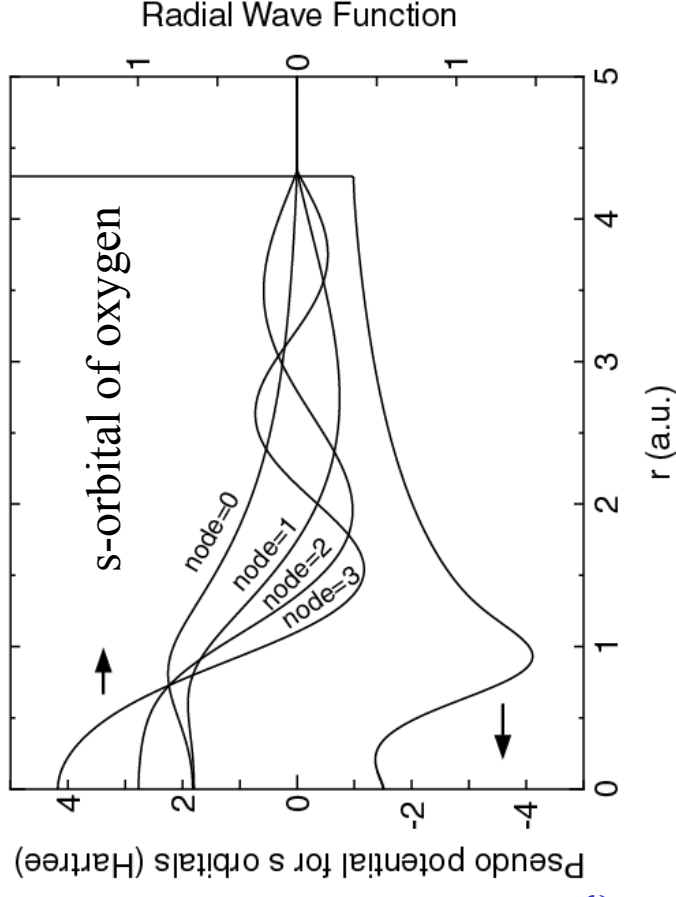
by an orbital optimization method

Primitive basis functions

1. Solve an atomic Kohn-Sham eq. under a confinement potential:

$$V_{\text{core}}(r) = \begin{cases} -\frac{Z}{r} & \text{for } r \leq r_1 \\ \sum_{n=0}^3 b_n r^n & \text{for } r_1 < r \leq r_c \\ h & \text{for } r_c < r, \end{cases}$$

2. Construct the norm-conserving pseudopotentials.
3. Solve ground and excited states for the pseudopotentials.

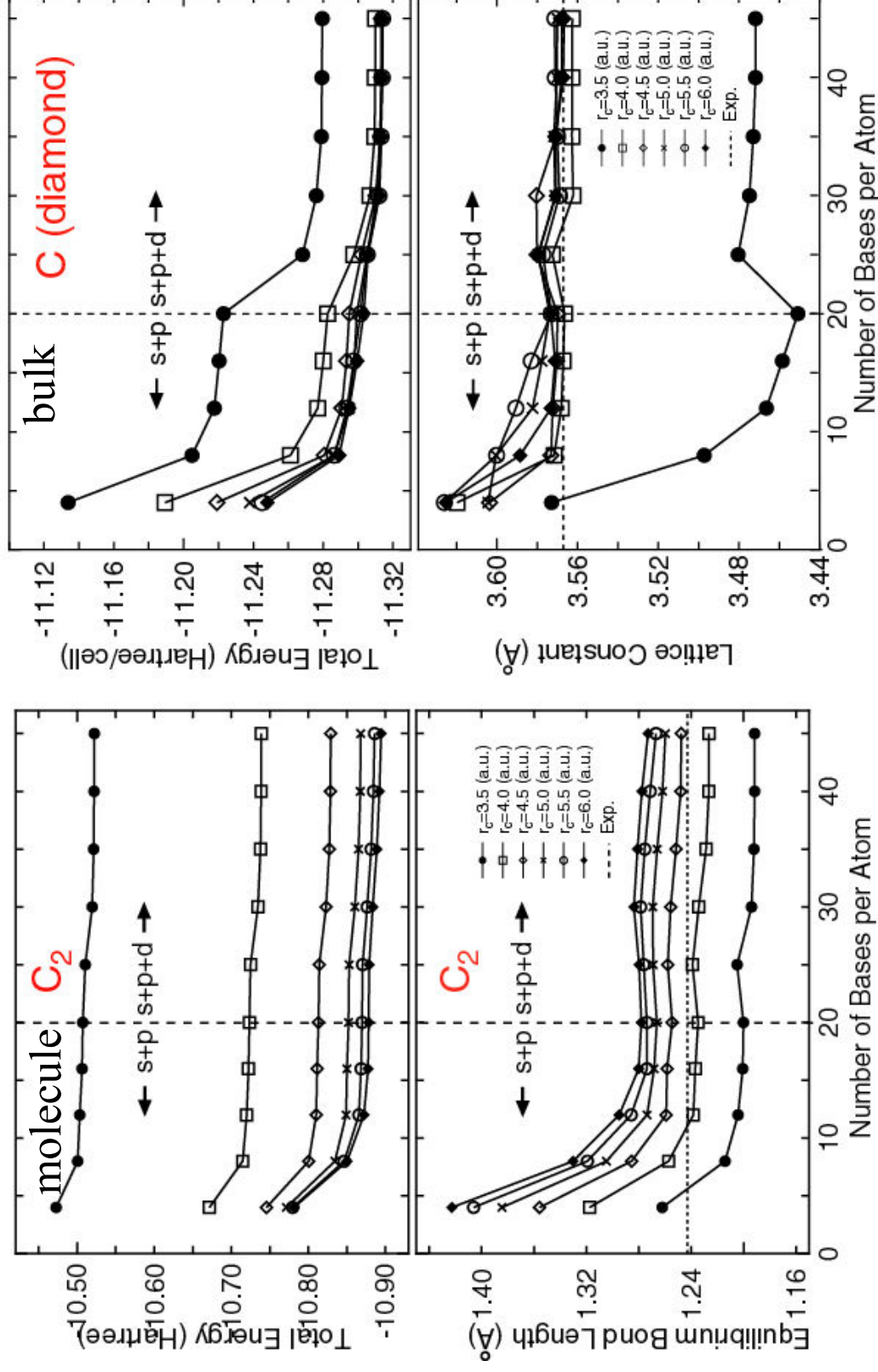


In most cases, the accuracy and efficiency can be controlled by

Cutoff radius
Number of orbitals

Convergence with respect to basis functions

The two parameters can be regarded as variational parameters.



Benchmark of primitive basis functions

Ground state calculations of dimer using primitive basis functions

Dimer	Expt.	Calc.	Dimer	Expt.	Calc.
H ₂ (H4.5-s2)	1Σ ⁺ _g a	1Σ ⁺ (1sσ _g ²)	K ₂ (K10.0-s2p2)	1Σ ⁺ _g f	1Σ ⁺ (3pπ _g ⁴ 3pσ _u ² 4sσ _g ²)
He ₂ (He7.0-s2)	1Σ ⁺ _g b	1Σ ⁺ (1sσ _g ² 1sσ _u ²)	CaO (Ca7.0-s2p2d2)	1Σ ⁺ _g k	1Σ ⁺ (sσ ² sσ ² pπ ⁴)
Li ₂ (Li8.0-s2)	1Σ ⁺ _g c	1Σ ⁺ (2sσ _g ²)	ScO (Sc7.0-s2p2d2)	2Σ ⁺ _g l	2Σ ⁺ (dπ ⁴ sσ ² sσ ¹)
BeO (Be6.0-s2p2)	1Σ ⁺ _g d	1Σ ⁺ (sσ ² sσ ² pπ ⁴)	Ti ₂ (Ti7.0-s2p2d2)	3Δ _g m	3Δ _g (4sσ _g ² 3dσ _g ¹ 3dπ _u ⁴ 3dδ ¹)
B ₂ (B5.5-s2p2)	3Σ ⁻ _g e	3Σ ⁻ (2sσ _g ² 2sσ _u ² 2π _u ²)	V ₂ (V7.5-s2p2d2)	3Σ ⁻ _g n	1Σ ⁺ (4sσ _g ² 3dσ _g ² 3dπ _u ⁴ 3dδ ²)
C ₂ (C5.0-s2p2)	1Σ ⁺ _g f	1Σ ⁺ (2sσ _g ² 2sσ _u ² 2π _u ⁴)	V ₂ (V7.5-s4p4d4f2)	3Σ ⁻ _g n	3Σ ⁻ (4sσ _g ² 3dσ _g ² 3dπ _u ⁴ 3dδ ²)
N ₂ (N5.0-s2p2)	1Σ ⁺ _g f	1Σ ⁺ (2sσ _g ² 2pπ _u ⁴ 2pσ _g ²)	Cr ₂ (Cr7.0-s2p2d2)	1Σ ⁺ _g o	1Σ ⁺ (4sσ _g ² 3dσ _g ² 3dπ _u ⁴ 3dδ ⁴)
O ₂ (O5.0-s2p2)	3Σ ⁻ _g f	3Σ ⁻ (2pσ _g ² 2pπ _u ⁴ 2pπ _g ²)	MnO (Mn7.0-s2p2d2)	6Σ ⁺ _g p	6Σ ⁺ (dσ ¹ dπ ⁴ dδ ² dπ ^{*2})
F ₂ (F5.0-s2p2)	1Σ ⁺ _g f	1Σ ⁺ (2pσ _g ² 2pπ _u ⁴ 2pπ _g ⁴)	Fe ₂ (Fe7.0-s2p2d2)	7Δ _u q	7Δ _u (4sσ _g ² 3dσ _g ² 3dσ _u ¹ 3dπ _u ⁴ 3dπ _g ² 3dδ _g ³ 3dδ _u ²)
Ne ₂ (Ne7.0-s2p2)	1Σ ⁺ _g g	1Σ ⁺ (2pπ _u ⁴ 2pπ _g ⁴ 2pσ _g ²)	Co ₂ (Co7.0-s2p2d2)	5Δ _g	5Δ _g (4sσ _g ² 3dσ _g ² 3dσ _u ¹ 3dπ _u ⁴ 3dπ _g ² 3dδ _g ⁴ 3dδ _u ³)
Na ₂ (Na9.0-s2p2)	1Σ ⁺ _g f	1Σ ⁺ (2pπ _g ⁴ 2pσ _u ² 3sσ _g ²)	Ni ₂ (Ni7.0-s2p2d2)	Ω ^r	3Σ ⁻ (4sσ _g ² 3dσ _g ² 3dσ _u ¹ 3dπ _u ⁴ 3dπ _g ² 3dδ _g ⁴ 3dδ _u ⁴)
MgO (Mg7.0-s2p2)	1Σ ⁺ _g h	1Σ ⁺ (sσ ² sσ ² pπ ⁴)	Cu ₂ (Cu7.0-s2p2d2)	1Σ ⁺ _g s	1Σ ⁺ (4sσ _g ² 3dσ _g ² 3dσ _u ¹ 3dπ _u ⁴ 3dπ _g ² 3dδ _g ⁴ 3dδ _u ⁴)
Al ₂ (Al6.5-s2p2)	3Π _u i	3Σ ⁻ (3sσ _g ² 3sσ _u ² 3pπ _u ²)	ZnH (Zn7.0-s2p2d2)	2Σ ⁺ _g t	2Σ ⁺ (sσ ² sσ ^{*1} dσ ² dπ ⁴ dδ ⁴)
Al ₂ (Al6.5-s4p4d2)	3Π _u i	3Σ ⁻ (3sσ _g ² 3sσ _u ² 3pπ _u ³)	GaH (Ga7.0-s2p2)	1Σ ⁺ _g u	1Σ ⁺ (sσ ² sσ ^{*2})
Si ₂ (Si6.5-s2p2)	3Σ ⁻ _g f	3Π _u f	GeO (Ge7.0-s2p2)	1Σ ⁺ _g v	1Σ ⁺ (ssσ ² spσ ² ppπ ⁴ ppσ ²)
Si ₂ (Si6.5-s2p2d1)	3Σ ⁻ _g f	3Σ ⁻ (3sσ _g ² 3pπ _u ² 3sσ _u ²)	As ₂ (As7.0-s2p2d1)	1Σ ⁺ _g f	1Σ ⁺ (4sσ _g ² 4sσ _u ² 4pσ _g ² 4pπ _u ⁴)
P ₂ (P6.0-s2p2d1)	1Σ ⁺ _g f	1Σ ⁺ (3sσ _g ² 3pσ _g ² 3pπ _u ⁴)	Se ₂ (Se7.0-s2p2d1)	3Σ ⁻ _g f	3Σ ⁻ (4sσ _g ² 4sσ _u ² 4pσ _g ² 4pπ _u ⁴ 4pπ _g ²)
S ₂ (S6.0-s2p2)	3Σ ⁻ _g f	3Σ ⁻ (3pσ _g ² 3pπ _u ⁴ 3pπ _g ²)	Br ₂ (Br7.0-s2p2d1)	1Σ ⁺ _g f	1Σ ⁺ (4sσ _g ² 4sσ _u ² 4pσ _g ² 4pπ _u ⁴ 4pπ _g ⁴)
Cl ₂ (Cl6.0-s2p2d2)	1Σ ⁺ _g f	1Σ ⁺ (3pσ _g ² 3pπ _u ⁴ 3pπ _g ⁴)	Kr ₂ (Kr7.0-s2p2)	1Σ ⁺ _g v	1Σ ⁺ (4sσ _g ² 4sσ _u ² 4pσ _g ² 4pπ _u ⁴ 4pπ _g ⁴)
Ar ₂ (Ar7.0-s2p2)	1Σ ⁺ _g j	1Σ ⁺ (3pπ _u ⁴ 3pπ _g ⁴ 3pσ _u ²)			

All the successes and failures by the LDA are reproduced by the modest size of basis functions (DNP in most cases)

Optimization of basis functions

Practically, the accuracy and efficiency can be controlled by

Number of basis functions

Cutoff radius

But, there is another one variational parameter:

Radial shape

If the radial shape can be optimized, it is expected that the high accuracy will be attainable with a small number of basis functions.

Variational optimization of basis functions No.1

One-particle wave functions

Contracted orbitals

$$\psi_{\mu}(\mathbf{r}) = \sum_{i\alpha} c_{\mu,i\alpha} \phi_{i\alpha}(\mathbf{r} - \mathbf{r}_i), \quad \phi_{i\alpha}(\mathbf{r}) = \sum_q a_{i\alpha q} \chi_{i\eta}(\mathbf{r}),$$

The variation of E with respect to \mathbf{c} with fixed \mathbf{a} gives

$$\frac{\partial E_{\text{tot}}}{\partial a} = 0 \quad \sum_{j\beta} \langle \phi_{i\alpha} | \hat{H} | \phi_{j\beta} \rangle c_{\mu,j\beta} = \varepsilon_{\mu} \sum_{j\beta} \langle \phi_{i\alpha} | \phi_{j\beta} \rangle c_{\mu,j\beta},$$

Regarding \mathbf{c} as dependent variables on \mathbf{a} and assuming KS eq. is solved self-consistently with respect to \mathbf{c} , we have

$$\begin{aligned} \frac{\partial E_{\text{tot}}}{\partial a_{i\alpha q}} &= \frac{\delta E_{\text{tot}}}{\delta \rho(\mathbf{r})} \frac{\delta \rho(\mathbf{r})}{\delta a_{i\alpha q}} \\ &= 4 \sum_{\mu} n_{\mu} \sum_{i\alpha,j\beta} c_{\mu,i\alpha} c_{\mu,j\beta} \left\langle \frac{\partial \phi_{i\alpha}}{\partial a_{i\alpha q}} | \hat{H} | \phi_{j\beta} \right\rangle + 4 \sum_{\mu} n_{\mu} \sum_{i\alpha,j\beta} \frac{\partial c_{\mu,i\alpha}}{\partial a_{i\alpha q}} c_{\mu,j\beta} \langle \phi_{i\alpha} | \hat{H} | \phi_{j\beta} \rangle \\ &= 2 \sum_{j\beta} \left(\Theta_{i\alpha,j\beta} \langle \chi_{i\eta} | \hat{H} | \phi_{j\beta} \rangle - E_{i\alpha,j\beta} \langle \chi_{i\eta} | \phi_{j\beta} \rangle \right), \end{aligned}$$

Variational optimization of basis functions No.2

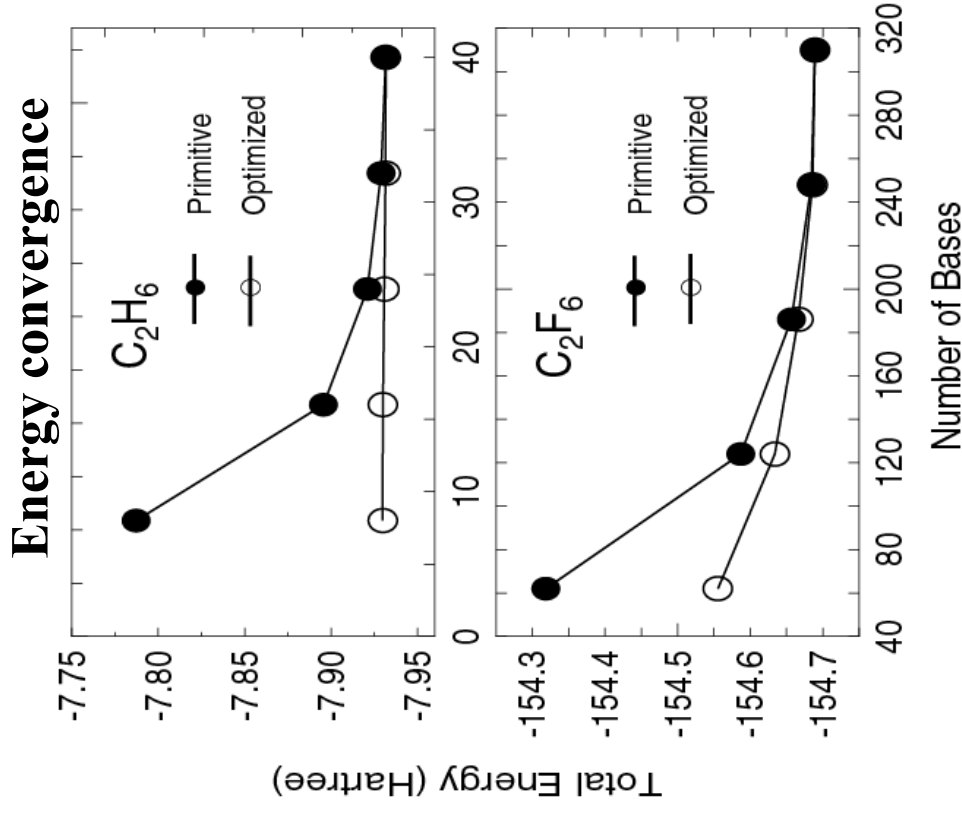
The basis functions can be optimized in the same procedure as for the geometry optimization.

Step 1 Self-consistently solving of Eq. (4),

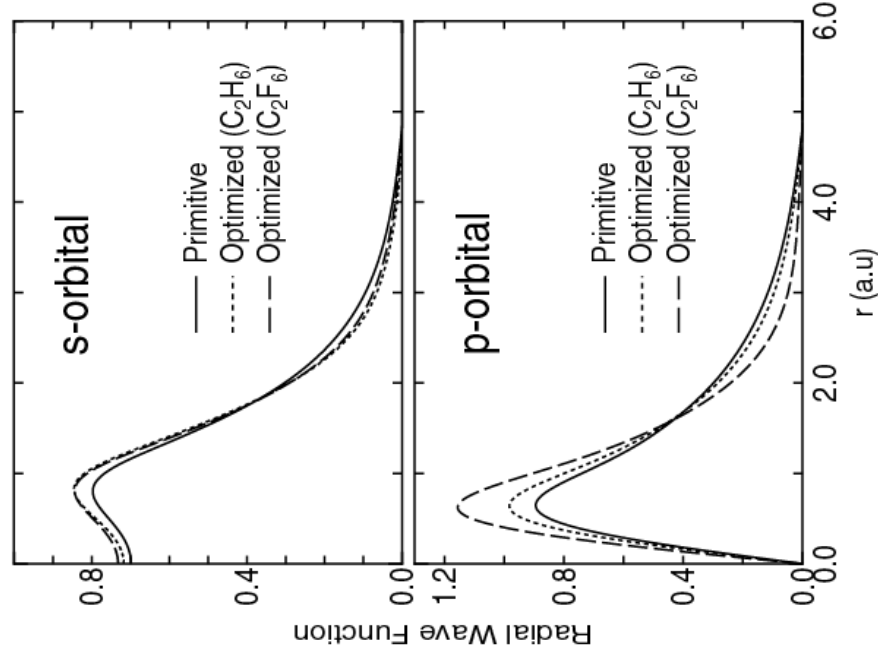
$$\text{Step 2 } a_{i\alpha q}^{(n+1)} = a_{i\alpha q}^{(n)} - \lambda \left(\frac{\partial E_{\text{tot}}}{\partial a_{i\alpha q}} \right)_{a^{(n)}},$$

$$n := n + 1,$$

Primitive vs. Optimized



Radial shape of carbon atom



Since the fluorine attracts electrons sitting p-orbitals of carbon, the p-orbital largely shrinks.

Notes in LCPAO

- **It is not a complete basis**
- **A modest accuracy is attainable in practical calculations**
- **The double valence plus a single polarization functions are an optimum choice.**
- **The use of many basis functions for dense bulk systems tends to be problematic due to the overcompleteness.**

RMM-DIIS for obtaining SCF

In most cases, the Residual Minimization Method in the direct Inversion of Iterative subspace (RMM-DIIS) in momentum space works well.

Residual vectors

$$R_n(\mathbf{q}) \equiv \rho_n^{(\text{out})}(\mathbf{q}) - \rho_n^{(\text{in})}(\mathbf{q}),$$

Kerker metric

$$\langle R_m | R_{m'} \rangle \equiv \sum_{\mathbf{q}} \frac{R_m^*(\mathbf{q}) R_{m'}(\mathbf{q})}{w(\mathbf{q})},$$

with the Kerker factor

$$w(\mathbf{q}) = \frac{|\mathbf{q}|^2}{|\mathbf{q}|^2 + q_0^2},$$

Let us assume the residual vector at the next step is expressed by

$$\bar{R}_{n+1} = \sum_{m=n-(p-1)}^n \alpha_m R_m,$$

Minimize

$$\langle \bar{R}_n | \bar{R}_n \rangle \longrightarrow \text{optimum } \alpha \text{ s}$$

with respect to α

Assume an optimum charge is given by

$$\rho_{n+1}^{(\text{in})} = \sum_{m=n-(p-1)}^n \alpha_m \rho_m^{(\text{in})} + \beta \sum_{m=n-(p-1)}^n \alpha_m R_m$$

Comparison of mixing methods

Anderson mixing

$$\bar{\rho}_n^{(\text{in})} = \rho_n^{(\text{in})} + \sum_{m=n-(p-1)}^{n-1} \theta_m (\rho_m^{(\text{in})} - \rho_n^{(\text{in})}). \quad \bar{R}_n^{(\text{in})} = R_n^{(\text{in})} + \sum_{m=n-(p-1)}^{n-1} \theta_m (R_m^{(\text{in})} - R_n^{(\text{in})}).$$

$\rho_{n+1}^{(\text{in})} = \bar{\rho}_n^{(\text{in})} + \beta \bar{R}_n^{(\text{in})} \rightarrow$ equivalent to RMM-DIIS

Broyden mixing

$$E = |G_n - G_{n-p}|^2 + \sum_{m=l+1-p}^{n-1} \langle \lambda_m | \{ (|n_{m+1}\rangle - |n_m\rangle) - G_n (|R_{m+1}\rangle - |R_m\rangle) \}$$

$$\frac{\partial E}{\partial G} = 0 \quad \frac{\partial E}{\partial \lambda} = 0$$

$$|n_{n+1}\rangle = |n_n\rangle - \sum_{m=n-p}^{n-1} \gamma_m^n (|n_{m+1}\rangle - |n_m\rangle) - G_{n-p} \left\{ |R_n\rangle - \sum_{m=n-p}^{n-1} \gamma_m^n (|n_{m+1}\rangle - |n_m\rangle) \right\}$$

$$G_{n-p} = -\beta \rightarrow \rho_{n+1}^{(\text{in})} = \bar{\rho}_n^{(\text{in})} + \beta \bar{R}_n^{(\text{in})} \rightarrow \text{equivalent to RMM-DIIS}$$

RMM-DIIS, Anderson, Broyden methods are all equivalent from the mathematical point of view and based on a quasi-Newton method.

A way for improving the SCF convergence

Broyden method

$$|n_{n+1}\rangle = |n_n\rangle - \sum_{m=n-p}^{n-1} \gamma_m^n (|n_{m+1}\rangle - |n_m\rangle) - G_{n-p} \left\{ |R_n\rangle - \sum_{m=n-p}^{n-1} \gamma_m^n (|n_{m+1}\rangle - |n_m\rangle) \right\}$$

$$G_{n-p} = -\beta \quad \longrightarrow \quad \rho_{n+1}^{(in)} = \bar{\rho}_n^{(in)} + \beta \bar{R}_n^{(in)}$$

If G can be stored, the Broyden method may be the best method among them. **However, G is too large to be stored.** Thus, from the theoretical point of view a reasonable improvement of the convergence can be obtained by increasing the number of of the previous steps.

In fact, the convergent results were obtained using 30-50 previous steps in the RMM-DIIS for 20 difficult systems that the SCF is hardly obtained using a smaller number of previous steps.

The results can be found in http://www.jaist.ac.jp/~t-ozaki/large_example.tar.gz

Geometry optimization

The geometry optimization in OpenMX is based on quasi Newton type optimization methods. Four kind of methods are available.

$$\mathbf{r}_{\text{new}} = \mathbf{r}_{\text{DIIS}} + \Delta\mathbf{r} \quad \Delta\mathbf{r} = -H^{-1} \mathbf{g}_{\text{DIIS}}$$

Treatment of H

DIIS **BFGS** **RF** (rational function) **EF** (eigenvector following)

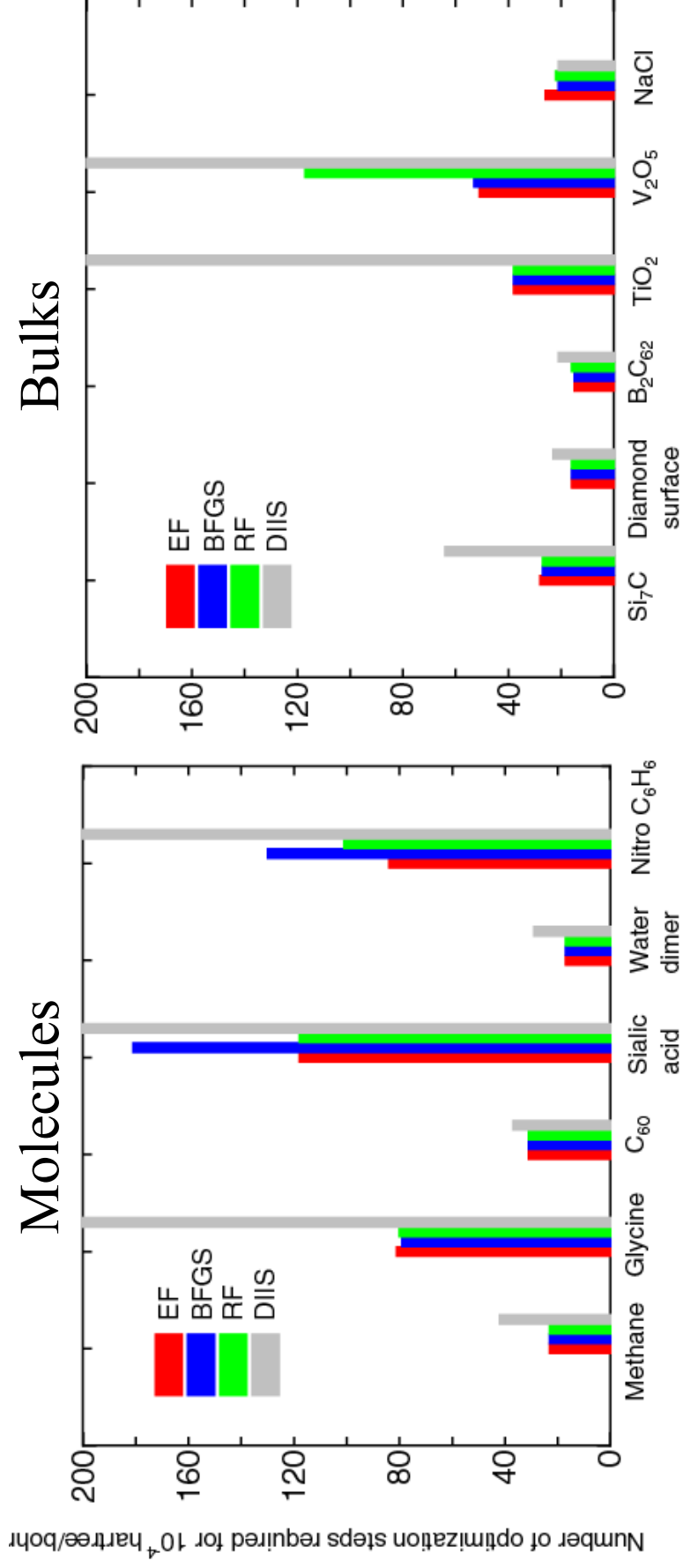
H=I BFGS BFGS+RF BFGS plus monitoring of eigenvalues of H

Broyden-Fletcher-Goldfarb-Shanno (BFGS) method

$$H_k = H_{k-1} + \frac{|\Delta\mathbf{g}_k\rangle\langle\Delta\mathbf{g}_k|}{\langle\Delta\mathbf{g}_k|\Delta\mathbf{r}_k\rangle} - \frac{|H_k\Delta\mathbf{r}_k\rangle\langle\Delta\mathbf{r}_k|H_k}{\langle\Delta\mathbf{r}_k|H_k|\Delta\mathbf{r}_k\rangle}$$

If the red part is positive, the positive definitiveness of H is kept.

The comparison of four quasi Newton methods



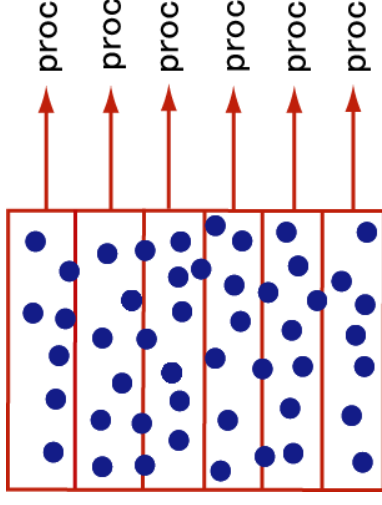
It turned out that the EF method is robust and efficient, while the RF also shows comparable performance.

The input files and out files used in the calculations shown in the figure can be found in "openmx3.3/work/geopt_example".

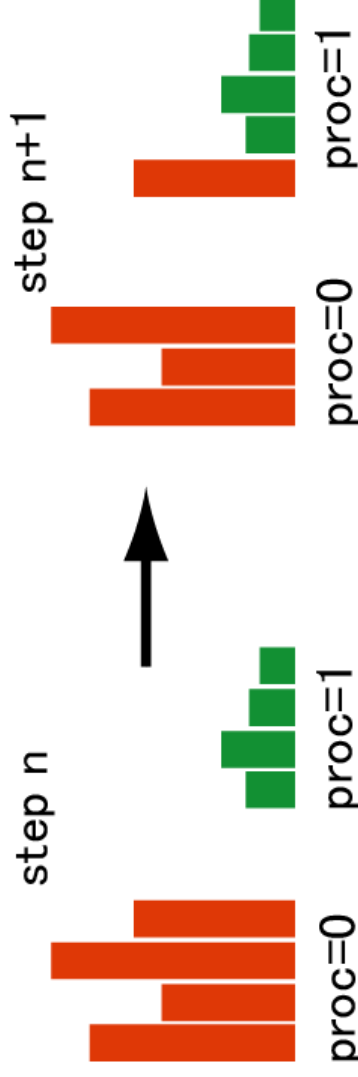
Parallelization

- The parallelization is basically done by a 1D-domain decomposition.
- Also a different parallelization scheme is considered depending on the data structure in each subroutine.
- The dynamic load balancing is attempted at every MD step.

1-D domain decomposition



Dynamic load balancing



Parallel efficiency

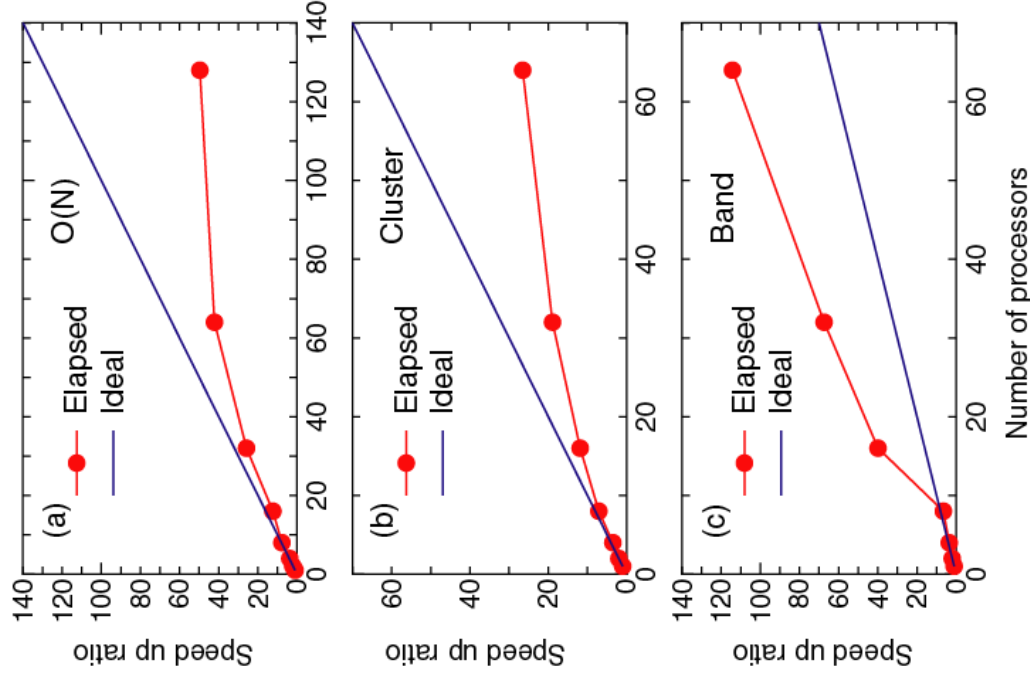
- (a) Diamond (512 atoms)
- (b) SMM (148 atoms)
- (c) Diamond (64 atoms,
k-points=3x3x3)

Cray-XT3

2.4 GHz

Interconnect

actual performance 1.0GB/s



The code

is written by a standard C, and consists of 800 subroutines, about 210000 lines, and is needed to include lapack, blas, fftw.

Main code: **openmx**

VPS and PAO generator: **adpack**

About ten post processing codes:

bandgnu13:	band disperion
dosMain:	DOS
jx:	exchange coupling constant
polB:	macroscopic polarization
esp:	analysis of charge state
.....	

How to handle the large software ?

The number of combination of parameters: $\propto 2^N$

Thus, it is not easy to assure the reliability of the code as the code becomes complicated.

In order to check the reliability of the most functionalities, several automatic testing systems have been developed:

- runtest:** a tester of installation and MPI
- mltest:** a tester of memory leak
- forcetest:** a tester of analytic forces
- filA3:** a checker of dynamic allocation

Ongoing and planned works

Ongoing

1. Hybrid parallelization using MPI and OpenMP by TO
2. Monkhorst-Pack k-points by H. Weng
3. Calculation of Wannier functions by H. Weng
4. Improvement of numerical integrations by TO
5. Release of NEGF by TO

Planned

1. Implementation of DMFT by J. Yu's group
2. Calculation of anomalous Hall effect by S. Onoda
3. Implementation of stress by TO
4. Refinement of pseudopotentials by TO
5. Implementation of hybrid functional by M. Toyoda

Summary

OpenMX is a state-of-the-art software package based on the local PAO basis functions and norm-conserving pseudopotentials.

The method can provide reasonable computational accuracy and efficiency in a balanced way for a wide variety of systems including solid state and molecular systems with careful consideration for the basis functions and pseudopotentials.

To improve the reliability and efficiency, and to add more functionalities, the code is still under development.